Journal of Controlled Release 336 (2021) 443–456

Contents lists available at ScienceDirect

Journal of Controlled Release

journal homepage: www.elsevier.com/locate/jconrel

Focused ultrasound with anti-pGlu3 Aβ enhances efficacy in Alzheimer's disease-like mice *via* recruitment of peripheral immune cells

Tao Sun [a,c,1], Qiaoqiao Shi [b,c,1], Yongzhi Zhang [a,c], Chanikarn Power [a,c], Camilla Hoesch [b], Shawna Antonelli [b], Maren K. Schroeder [b], Barbara J. Caldarone [d], Nadine Taudte [e], Mathias Schenk [e], Thore Hettmann [f], Stephan Schilling [e,f,g], Nathan J. McDannold [a,c,2,*], Cynthia A. Lemere [b,c,2,*]

[a] *Focused Ultrasound Laboratory, Department of Radiology, Brigham and Women's Hospital, 75 Francis Street, Boston, MA, United States of America*
[b] *Ann Romney Center for Neurologic Diseases in the Department of Neurology, Brigham and Women's Hospital, 75 Francis Street, Boston, MA, United States of America*
[c] *Harvard Medical School, Boston, MA, United States of America*
[d] *Harvard Medical School Mouse Behavior Core, Boston, MA, United States of America*
[e] *Fraunhofer Institute for Cell Therapy and Immunology, Department Molecular Drug Biochemistry and Therapy, Halle (Saale), Germany*
[f] *Vivoryon Therapeutics AG, Halle (Saale), Germany*
[g] *Anhalt University of Applied Sciences, Köthen, Germany.*

ARTICLE INFO

Keywords:
Focused ultrasound
Blood brain barrier
Drug delivery
Pyroglutamate-3 amyloid-β
Alzheimer's disease

ABSTRACT

Pyroglutamate-3 amyloid-β (pGlu3 Aβ) is an N-terminally modified, pathogenic form of amyloid-β that is present in cerebral amyloid plaques and vascular deposits. Here, we used focused ultrasound (FUS) with microbubbles to enhance the intravenous delivery of an Fc-competent anti-pGlu3 Aβ monoclonal antibody, 07/2a mAb, across the blood brain barrier (BBB) in an attempt to improve Aβ removal and memory in aged APP/PS1dE9 mice, an Alzheimer's disease (AD)-like model of amyloidogenesis.

First, we demonstrated that bilateral hippocampal FUS-BBB disruption (FUS-BBBD) led to a 5.5-fold increase of 07/2a mAb delivery to the brains compared to non-sonicated mice 72 h following a single treatment. Then, we determined that three weekly treatments with 07/2a mAb alone improved spatial learning and memory in aged, plaque-rich APP/PS1dE9 mice, and that this improvement occurred faster and in a higher percentage of animals when combined with FUS-BBBD. Mice given the combination treatment had reduced hippocampal plaque burden compared to PBS-treated controls. Furthermore, synaptic protein levels were higher in hippocampal synaptosomes from mice given the combination treatment compared to sham controls, and there were more CA3 synaptic puncta labeled in the APP/PS1dE9 mice given the combination treatment compared to those given mAb alone. Plaque-associated microglia were present in the hippocampi of APP/PS1dE9 mice treated with 07/2a mAb with and without FUS-BBBD. However, we discovered that plaque-associated Ly6G+ monocytes were only present in the hippocampi of APP/PS1dE9 mice that were given FUS-BBBD alone or even more so, the combination treatment. Lastly, FUS-BBBD did not increase the incidence of microhemorrhage in mice with or without 07/2a mAb treatment.

Our findings suggest that FUS is a useful tool to enhance delivery and efficacy of an anti-pGlu3 Aβ mAb for immunotherapy either *via* an additive effect or an independent mechanism. We revealed a potential novel mechanism wherein the combination of 07/2a mAb with FUS-BBBD led to greater monocyte infiltration and recruitment to plaques in this AD-like model. Overall, these effects resulted in greater plaque removal, sparing of synapses and improved cognitive function without causing overt damage, suggesting the possibility of FUS-BBBD as a noninvasive method to increase the therapeutic efficacy of drugs or biologics in AD patients.

* Corresponding authors at: Brigham and Women's Hospital, Harvard Medical School, 75 Francis Street, Boston, MA, United States of America.
E-mail addresses: njm@bwh.harvard.edu (N.J. McDannold), clemere@bwh.harvard.edu (C.A. Lemere).
[1] Co-first authors.
[2] Co-senior authors.

https://doi.org/10.1016/j.jconrel.2021.06.037
Received 14 January 2021; Received in revised form 22 June 2021; Accepted 24 June 2021
Available online 26 June 2021

1. Introduction

Alzheimer's disease (AD), the most common form of dementia worldwide, is defined pathologically by the presence extracellular amyloid-β (Aβ) plaques and intracellular neurofibrillary tangles containing hyperphosphorylated tau in the brain [1]. While Aβ peptide occurs as a monomer under normal conditions, small neurotoxic aggregates, known as soluble Aβ oligomers, accumulate and aggregate further to form amyloid plaques [1,2]. Increased Aβ production and reduced clearance are thought to underly the gradual accumulation of aggregated Aβ in AD brain [3]. Passive immunization approaches of anti-Aβ immunotherapy have been used for boosting Aβ clearance in mouse models and humans. However, limited delivery of antibodies, systematic side effects due to the off-target effects, and high cost have been handicaps for effective usage of these strategies in clinical trials [4,5]. One of the main obstacles of effective drug delivery to the central nervous system is the blood brain barrier (BBB), a semipermeable barrier comprised of endothelial cells, astrocytes and pericytes, that protects the brain by blocking entry of circulating toxins [6]. Unfortunately, the BBB also limits CNS penetration of drugs into brain [7,8].

Here, we investigated an alternative approach to conventional anti-Aβ immunotherapy that facilitates enhanced and spatially targeted modulation of Aβ clearance in order to establish a more precise and controlled treatment paradigm for AD. To enhance the antibody delivery and Aβ clearance in a targeted manner, we used microbubble (MB)-enhanced focused ultrasound (FUS) to open the blood-brain barrier (BBB) noninvasively, reversibly and repeatedly [9,10]. In this process, intravenously (i.v.) injected preformed microbubbles concentrate mechanical forces and stresses onto the vasculature. These mechanical effects result in an increased permeability of the BBB that lasts for several hours. MB-enhanced FUS has been reported previously to enable delivery of exogenous anti-Aβ antibodies [11,12] and a GSK-3 inhibitor [13] in AD transgenic (Tg) mouse models and reduce plaque burden. Other studies have shown that ultrasound-induced BBB opening itself improved Aβ clearance and behavior in 4 month-old [14], 7 month-old [15], 1 year-old [16], and 2 year-old [17] AD-like Tg mouse models. Increased neuronal plasticity with more newborn neurons [15] and microglial activation [14,16] were also observed. A clinical trial on MB-enhanced FUS (alone) in AD patients has begun [18].

Amyloid-Related Imaging Abnormalities (ARIA) are transient vascular adverse events, including vasogenic edema and microhemorrhage, that have been observed in anti-amyloid immunotherapy clinical trials, especially in individuals with pre-existing amyloid deposition in blood vessel walls, a condition known as congophilic amyloid angiopathy (CAA). It remains unclear whether FUS-mediated enhanced delivery of an anti-Aβ monoclonal antibody (mAb) in aged AD Tg mice with both plaque and vascular amyloid will be effective or if increasing antibody delivery to the brain will augment the incidence of microhemorrhage. In addition, the potential role of FUS in sparing synapse loss, an early pathological signature of cognitive decline in AD, is not well understood. We hypothesized that combining FUS-mediated BBB disruption (FUS-BBBD) with anti-Aβ immunotherapy targeting a pathogenic form of amyloid may further enhance the immunotherapeutic effects *via* increased and localized passive delivery of immunotherapy agents as well as the recruitment and activation of immune cells which may facilitate plaque removal.

Pyroglutamate-3 Aβ (pGlu3 Aβ) is a pathogenic, toxic form of amyloid-β that is present in many plaques and vascular amyloid in human brain and AD-like amyloid Tg mouse models [19]. To our knowledge, this is the first study to use FUS-BBBD to target pGlu3 Aβ as a treatment for AD. Our rationale for using an anti-pGlu3 Aβ mAb is that pGlu3 Aβ is a pathogenic form of Aβ that is only found in brain and correlates with disease progression. Unlike other anti-Aβ mAbs that bind unmodified Aβ in the brain and blood, there is no detectable pGlu3 Aβ in the periphery, therefore more mAb is available to get into brain. In addition, the antibody only binds a pathogenic form and therefore, does not block normal physiological properties of Aβ or its precursor, APP. We obtained a murine anti-pGlu3 amyloid-β IgG2a mAb (07/2a mAb) from Vivoryon Therapeutics AG (Halle, Germany) for this study. We previously characterized and determined the pathological efficacy *in vivo* and *ex vivo* as well as *in vivo* behavioral improvement using 07/2a mAb and its IgG1 version, 07/1, in APP/PS1dE9 Tg mice, a model of Alzheimer's disease amyloidosis [20–23]. Here, we investigated whether FUS-BBBD combined with the anti-pGlu3 Aβ 07/2a mAb can improve clearance of amyloid plaques and cognition in aged APP/PS1dE9 mice without increasing the incidence of microhemorrhage. Additionally, pathological assessments including synapse density, monocyte infiltration, and the presence of plaque-associated gliosis were performed to elucidate potential mechanisms of the combination therapy effects.

2. Results

2.1. FUS system and the reliable disruption of BBB

A system to perform FUS-induced BBB disruption in mice without MRI guidance was assembled in a non-barrier facility where the animals undergo behavior testing (Fig. 1a). An 835-kHz FUS transducer was used to apply pulsed sonications (10-ms bursts at 2 Hz for 100 s) on two hippocampal targets in each hemisphere in conjunction with 100 μl/kg i.v. injections of Optison™ MBs. We conducted a pilot study to confirm that we could reliably target the hippocampus with this system. This confirmation was made with fluorescent images of Trypan blue delivery (Fig. 1c).

2.2. FUS-BBBD increased delivery of anti-pGlu3 Aβ mAb

In order to determine whether FUS-BBBD affected antibody delivery to brain, we injected 300 μg of the anti-pGlu3 Aβ mAb i.v. with or without BBB disruption in 24–30 month-old APP/PS1dE9 mice and measured the mAb concentration (Fig. 1d) in the brain by ELISA 72 h later. FUS-BBBD enabled a 5.5-fold enhancement in mAb delivery into the brain. In APP/PS1dE9 mice given the combination treatment (Tg: mAb + FUS) ($n = 5$), the mean concentration was 173.0 pg mAb per mg brain, significantly higher ($p = 0.019$) than the 31.5 pg mAb per mg brain measured in the APP/PS1dE9 mice given 07/2a mAb alone (Tg: mAb controls) (n = 5).

2.3. Enhanced cognitive improvement in APP/PS1dE9 mice with combined anti-pGlu3 Aβ mAb and FUS-BBBD treatment

In another study, 16 month-old male APP/PS1dE9 mice were treated with i.v. infusion of pGlu3 Aβ mAb alone or immediately before FUS-BBBD in three weekly sessions, followed a week later by behavior tests, euthanasia and tissue harvest at ~17.5 months of age (Fig. 1b). We assessed learning and memory in 17 month-old WT mice treated with PBS (WT:PBS) or FUS-BBBD alone (WT:FUS), and APP/PS1dE9 mice treated with PBS (Tg:PBS), FUS-BBBD alone (Tg:FUS), mAb alone (Tg: mAb), and mAb combined with FUS-BBBD (Tg:mAb + FUS). We used the Water T Maze (WTM) test, which measures spatial cognition during the animal's learning and memory of the platform location [24]. Mice in the Tg:PBS group showed significant impairment in finding the platform over days 2–8 of testing compared to the mice in the WT:PBS group ($p < 0.05$; Fig. 2a). Mice in the WT:FUS group performed similarly to the WT: PBS animals and significantly better than Tg:PBS animals on days 3–8 ($p < 0.05$; Fig. 2a). The performance of the Tg:mAb + FUS mice was significantly better than that of the Tg:PBS mice on days 5–8 ($p < 0.05$; Fig. 2a). The improvement began one day later in the Tg:mAb group and was significant compared to Tg:PBS animals on days 6–8 ($p < 0.05$; Fig. 2a).

We also compared the percentage of animals that correctly learned the platform location in the WTM test at least 80% of the time for two consecutive days (Fig. 2b). The percentage of the Tg:PBS mice that

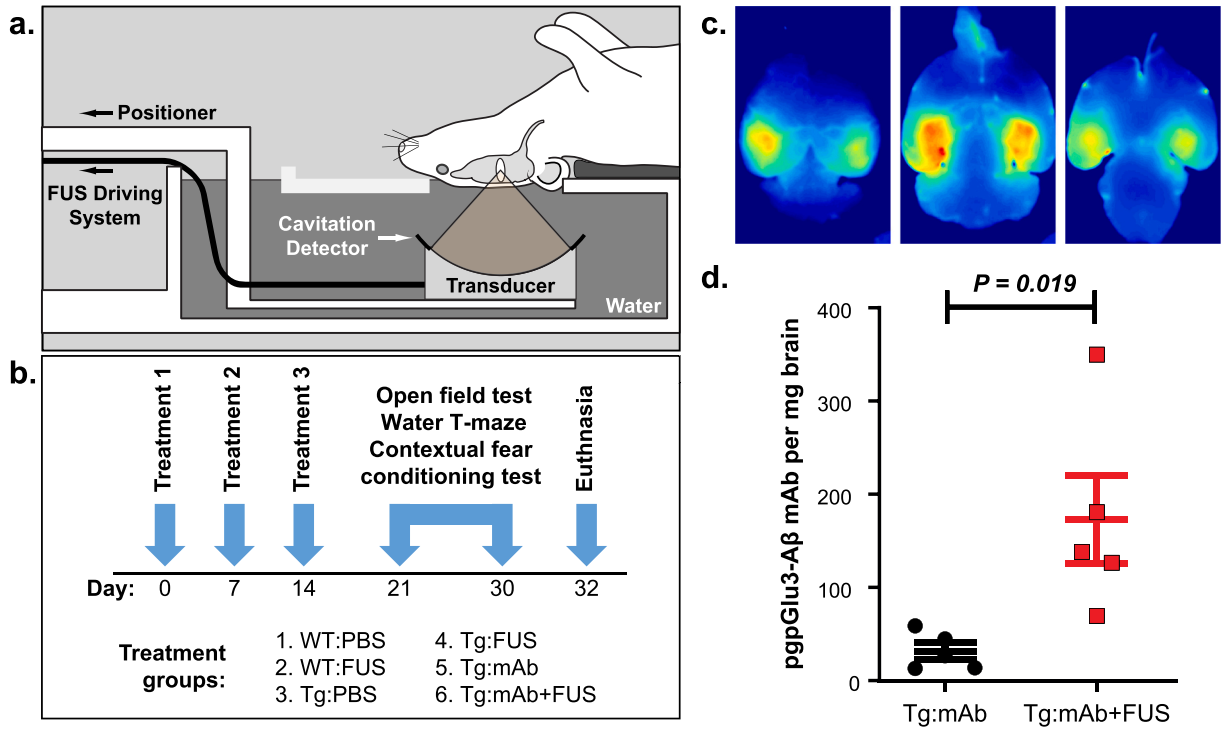

Fig. 1. Treatment paradigm and fluorescent imaging of bilateral Trypan Blue delivery to the hippocampus. a. Male APP/PS1dE9 mice at 16 months of age or wildtype (WT) age-matched male C57BL/6 J mice were placed supine above the FUS transducer, which was positioned so that the focus was centered on the hippocampus. b. The mice were divided into 6 groups that received treatment with intravenous PBS, intravenous anti-pGlu3 Aβ mAb (07/2a), or intravenous anti-pGlu3 Aβ mAb immediately before BBB disruption *via* intravenous MB infusion and FUS-mediated BBBD. Mice were treated weekly for 3 weeks. Behavioral testing started 1 week after the final treatment and lasted 11 days, after which mice were sacrificed and tissue was collected for analysis. c. Fluorescence imaging of Trypan Blue delivery in a mouse brain after BBB disruption *via* MB-enhanced FUS. Two targets were sonicated in the hippocampus in each hemisphere in a pilot study to confirm the targeting accuracy of the system. After euthanasia and transcardial perfusion, the brain was cut into 2 mm slabs. The BBB disruption covered the hippocampus bilaterally and extended the full dorsal/ventral axis of the brain. d. Concentration of pGlu3-Aβ mAb (07/2a) in controls and sonicated 24–30 month APP/PS1dE9 mice 72 h after i.v. mAb administration ($n = 5$/group). BBB disruption resulted in a significant 5.5-fold increase in mAb concentration in brain (Student *t*-test). (For interpretation of the references to colour in this figure legend, the reader is referred to the web version of this article.)

reached this predetermined criterion by day 8 was only 11% (1/9), indicating that they were unable to learn the task (Fig. 2b). Hence, the reversal test was not conducted in this study. At the end of the 8 days, all animals in the WT:FUS (6/6) and Tg:mAb + FUS (5/5) groups reached this criterion, while 70% (7/10), 71% (5/7), and 67% (6/9) of the WT:PBS, Tg:FUS, and Tg:mAb mice reached it, respectively. We compared the number of days required to reach this predetermined criterion (Fig. 2c). For this comparison, we assumed the best-case scenario where animals that did not reach this criterion at day 8 did so immediately after our tests on day 9 (if 80% correct or higher on day 8) or 10 (if less than 80% correct on day 8). The days required to reach criterion for the WT:PBS, WT:FUS, and Tg:mAb + FUS groups was significantly less ($p < 0.05$) than the Tg:PBS group. The days required by the Tg:FUS and Tg:mAb groups were not significantly better than the Tg:PBS mice. Overall, the WTM results show that the anti-pGlu3 Aβ mAb alone was effective in improving learning and memory in these aged APP/PS1dE9 mice, and that this improvement occurred faster and in a higher percentage of animals when combined with three weekly treatments with FUS-BBBD.

2.4. No significant effects in fear learning and memory or locomotor activity with anti-pGlu3 Aβ mAb or FUS-BBBD

In the Contextual Fear Conditioning test (CFC), we did not observe a significant difference between the WT:PBS and the Tg:PBS groups in post-shock freezing time during the training period on day 1 (fear learning), or the freezing time in the absence of shock in the same box on day 2 (fear memory), suggesting that either the Tg mice were not deficient in this test or that the study was underpowered to see a significant difference. During the training on day 1, mice in the WT:FUS group had significantly increased freezing times ($p < 0.05$) following the first shock compared to the Tg:PBS group and following the second shock compared to Tg:PBS and Tg:mAb groups. We saw no significant differences between groups in the Context test on day 2. In addition, no significant differences were seen between groups in the distance traveled in the Open Field test. Overall, these results show that FUS, anti-pGlu3 Aβ mAb, or their combination did not grossly impact fear learning or fear memory in CFC tests or locomotor activity or anxiety in the Open Field test.

2.5. Decreased hippocampal plaque deposition in APP/PS1dE9 mice co-treated with anti-pGlu3 Aβ mAb and FUS-BBBD

To determine whether the spatial memory improvement we observed in the APP/PS1dE9 mice with the combination of FUS-BBBD and 07/2 treatment was associated with decreased Aβ in the sonicated hippocampal targets, we examined the Aβ plaque load in the hippocampus and in the non-sonicated pre-frontal cortex (PFC) in the Tg mice (Fig. 3). A significant decrease in Aβx-42 plaque deposition in the hippocampus was found in the Tg:mAb + FUS mice ($p < 0.05$, Fig. 3a, b). No significant differences in Aβx-42 plaque burden were observed between mice treated with PBS, 07/2a alone, or FUS alone (Fig. 3a-e). In addition, no significant difference was observed between any group in Aβx-42 plaque deposition in the PFC or in Aβx-40 plaque deposition in the hippocampus or PFC. PyroGlu3 Aβ plaque deposition in the hippocampus was reduced in both the Tg:mAb and the Tg:mAb + FUS groups but only reached significance in the Tg:mAb + FUS group compared to the PBS-

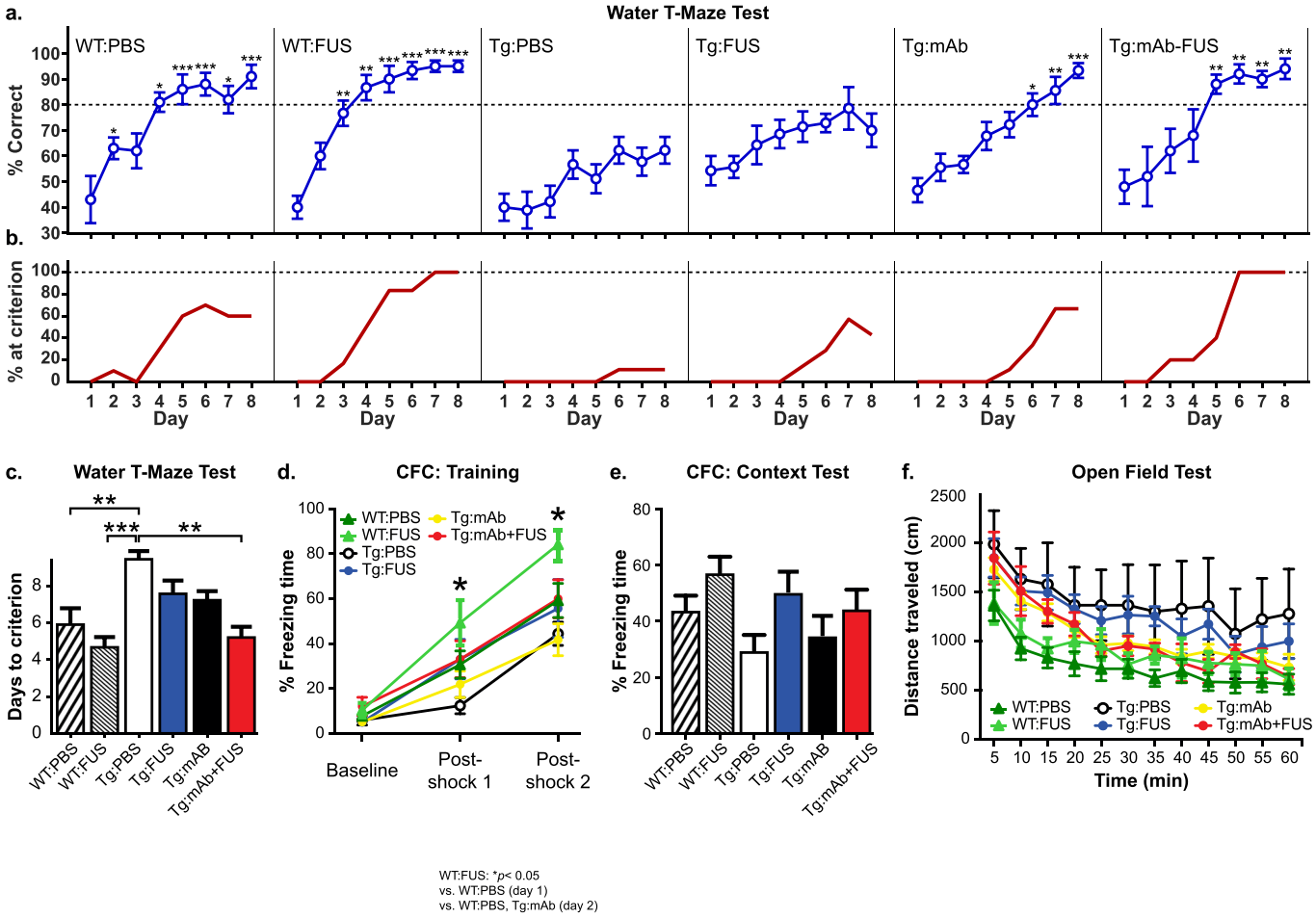

Fig. 2. Behavior tests in WT and Tg mice with or without FUS-BBBD and pGlu3 Aβ mAb, 07/2a. a. Tg:PBS mice were significantly impaired in the Water T Maze (WTM) test compared to WT:PBS and WT-FUS mice at 17 months of age starting at day 2 and 3, respectively. The Tg:mAb and Tg:mAb + FUS groups showed significantly improved spatial learning and memory in the WTM compared to the Tg:PBS group. The Tg:mAb + FUS group reached significance at day 5, one day before the Tg:mAb mice; by day 8, the scores in these two treatment groups were both similar to the performance of WT mice treated with PBS or FUS (repeated measures ANOVA followed by Tukey's post-hoc test, $*p < 0.05$; $**p < 0.01$; $*** p < 0.001$ compared to Tg:PBS at each day). b. Percent of mice that reached a pre-defined criterion (≥ 80% correct choices on 2 consecutive days) in the WTM test. At the end of the 8 days, all animals in the WT:FUS (6/6) and Tg:mAb + FUS (5/5) groups reached this criterion, while 70% (7/10), 71% (5/7), and 67% (6/9) of the WT:PBS, Tg:FUS, and Tg:mAb mice did, respectively. c. The WT:PBS, WT:FUS, and Tg:mAb + FUS groups required significantly fewer days on average to reach this criteria than the Tg:PBS animals. d. In Context Fear Conditioning (CFC), WT:FUS mice spent significantly more time freezing after the first shock than the Tg:PBS group and after the second shock compared to the Tg:PBS and Tg:mAb groups. e. No significant differences among groups was observed in the CFC Context test (e), or in analyses of locomotor activity, distance traveled (f). (WT:PBS, $n = 10$; WT:FUS, $n = 6$; Tg:PBS, $n = 8–9$; Tg:FUS, $n = 7$; Tg:mAb, n = 8–9; Tg:mAb + FUS, n = 5–6; one-way ANOVA followed by Tukey's post-hoc test, $*p < 0.05$; $**p < 0.01$; $*** p < 0.001$).

treated mice (Fig. 3f, g). No significant differences in pGlu3 Aβ plaque deposition were seen in PFC (Fig. 3h), indicating that the effect was localized to the sonicated area. Immunostaining with an anti-mouse IgG2a secondary antibody alone to detect 07/2a in mouse brain sections revealed similar patterns between groups 3 weeks after the last treatment (data not shown).

ELISA measurements of Aβ in homogenates from whole mouse hemibrains revealed no significant differences in guanidine-soluble (Tper insoluble) Aβx-42 and Aβx-40 levels between groups (Fig. 3i, j). These results are not surprising given the hippocampal targeting of FUS-mediated BBBD and the short treatment period. However, plaque-lowering in hippocampus suggests that combining the pGlu-Aβ mAb with FUS-BBBD exerted an additive effect to reduce Aβ plaque deposition in the sonicated hippocampus of APP/PS1dE9 mice.

2.6. Age-related hippocampal synaptic degeneration is reduced in APP/PS1dE9 mice after treatment with 07/2a and FUS-BBBD

Previous reports have demonstrated that aging in APP/PS1 mice is associated with reductions is synapse number as well as the levels of synaptic proteins and mRNA in the hippocampus and cortex [25–28]. To determine the effects of FUS and 07/2a on hippocampal synapses in aged APP/PS1dE9 mice, we performed high resolution confocal microscopy analysis [28] of pre- and post-synaptic markers (i.e. synaptic puncta) in hippocampal CA3 in mice treated with mAb alone in combination with FUS-BBBD. The mice in the Tg:mAb + FUS group had significantly more Vglu2-positive ($p < 0.01$), GluR1-positive ($p < 0.01$) and colocalized synaptic puncta ($p < 0.01$) than APP/PS1dE9 mice treated with 07/2a alone (Fig. 4a, b). Western blotting of pre-synaptic markers, Vglut2 and Synapsin-1 (SYN-1), and post-synaptic markers, GluR1 and PSD95, in hippocampal synaptosomes showed significantly elevated synaptic protein levels in mice in the Tg:mAb + FUS group compared to the Tg:PBS or Tg:FUS animals ($p < 0.01$, Fig. 4c, d). The

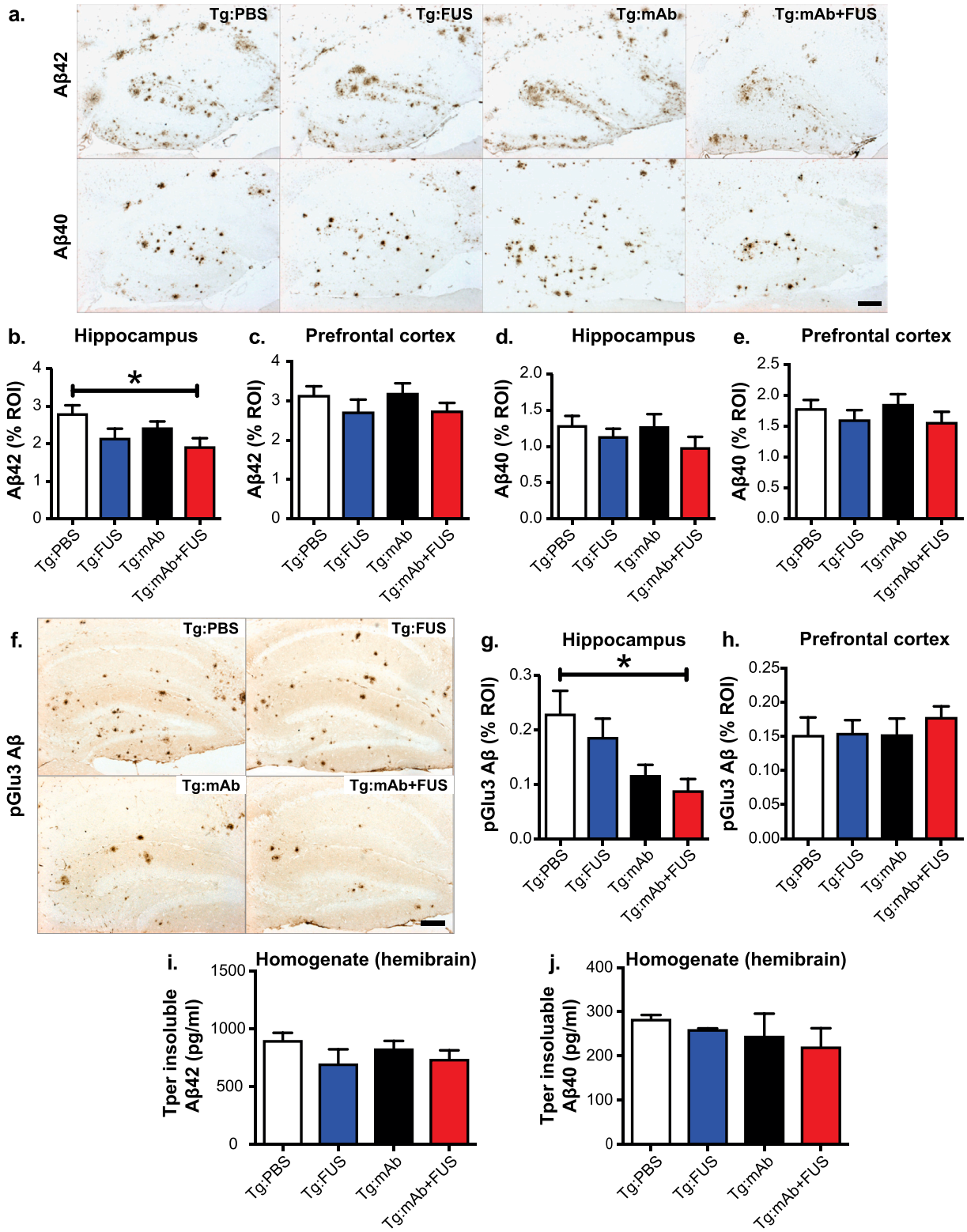

Fig. 3. Aβ plaque load in 17.5 month-old Tg mice treated with PBS, FUS, anti-pGlu3 Aβ mAb, or a combination of mAb and FUS. a-e. Aβ42 immunoreactivity within the region-of-interest (ROI) showed reduced plaque burden in mice in the Tg:mAb + FUS group vs. Tg:PBS group (a, top row). No such reduction was observed in sections stained for Aβ40 immunoreactivity (a, bottom row). Quantification of the area of Aβ42-positive plaques showed a significant lowering in the hippocampus (b), but not the prefrontal cortex (PFC, c), in mice in the Tg:mAb + FUS group compared to mice in the Tg:PBS group. No significant difference among treatment groups was observed in the area of Aβ40 plaques in either hippocampus (d) or PFC (e). Scale bar = 100 μm. f-h. pGlu3 Aβ immunoreactivity in sections stained with K17 showed significantly decreased plaque load in the hippocampus RO1 in mice in the Tg:mAb + FUS group compared mice in the Tg:PBS group (f, g). No significant difference was found in pGlu3-Aβ immunoreactivities in the PFC (h). Scale bar = 100 μm. i-j. No significant differences were seen in Aβ42 and Aβ40 levels by ELISA in whole hemibrain homogenates. (Tg:PBS, $n = 9$; Tg:FUS, $n = 7$; Tg:mAb, n = 9; Tg:mAb + FUS, $n = 6$; one-way ANOVA followed by Tukey's pos-thoc test; (*$p < 0.05$).

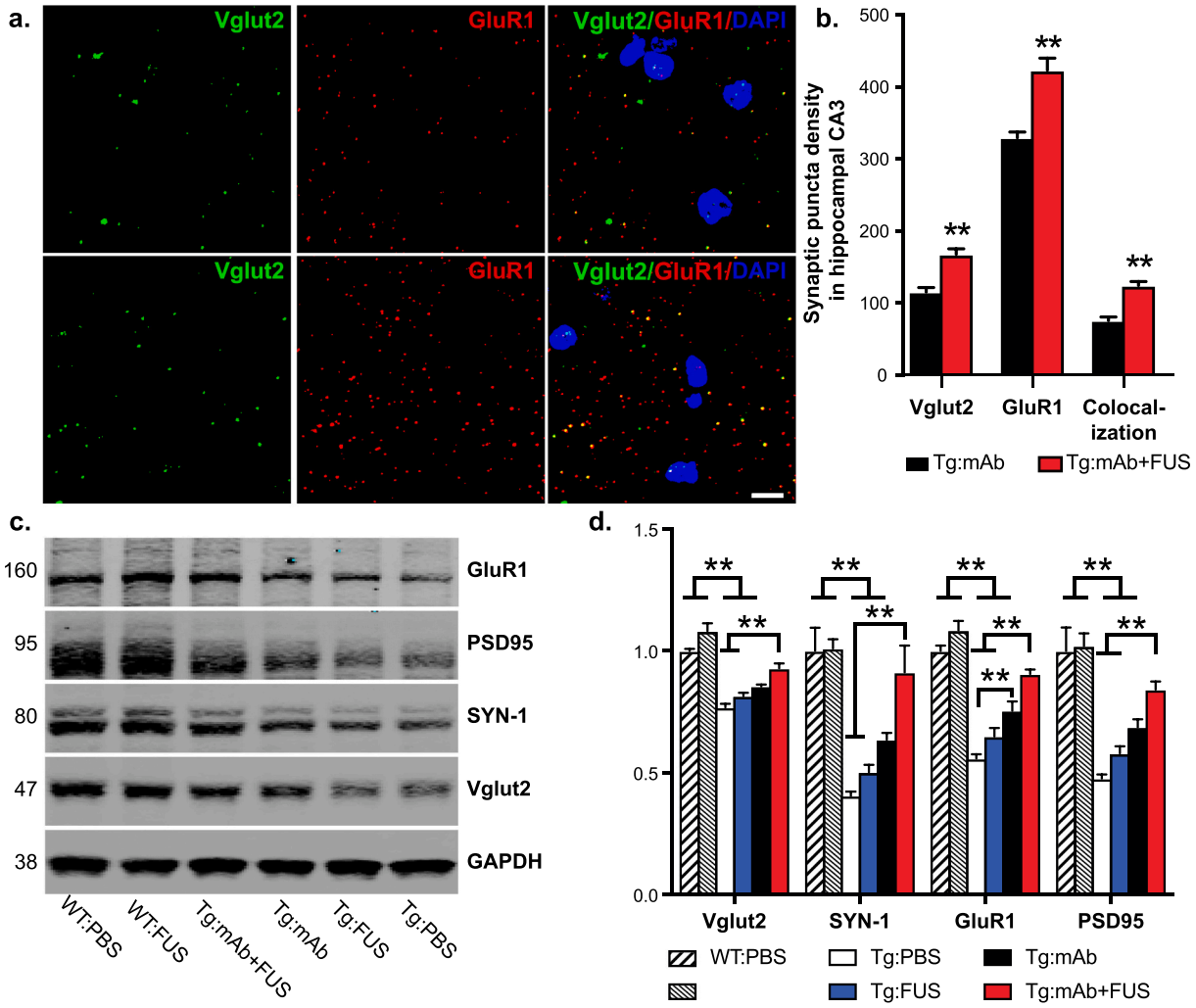

Fig. 4. Synaptic puncta analysis and synaptic protein levels in 17.5 month old mice with or without FUS-BBBD and pGlu3 Aβ mAb. a. Synaptic puncta of pre-synaptic and post-synaptic markers Vglut2 and GluR1, respectively, and their colocalization in hippocampal CA3 were analyzed by high resolution confocal microscopy in Tg mice treated with mAb alone or in combination with FUS-BBBD. Scale bar = 5 μm. b. Mice in the Tg:mAb + FUS group showed increased Vglut1, GluR1 and co-localized synaptic densities compared to the Tg:mAb mice (** $p < 0.01$, 3 equidistant planes, 300 μm apart; Student t-test). c-d. Western blotting of synaptic proteins in hippocampal synaptosomes isolated from WT and Tg mice indicated increased levels of the pre-synaptic proteins Vglut2 and SYN-1 and the post-synaptic proteins GluR1 and PSD95 in the Tg:mAb + FUS mice compared to the Tg:PBS and Tg:FUS groups, suggesting a sparing of synaptic loss resulting from the combination of mAb and FUS-BBBD. (WT:PBS, $n = 13$; WT:FUS, $n = 8$; Tg:PBS, n = 9; Tg:FUS, n = 7; Tg:mAb, n = 9; Tg:mAb + FUS, n = 6; one-way ANOVA followed by Tukey's post-hoc test, **$p < 0.01$).

animals in the Tg:mAb group had increased GluR1 compared to the Tg:PBS mice ($p < 0.01$, Fig. 4c, d), but such differences were not found for the other synaptic proteins. WT mice that received PBS only or FUS-BBBD showed significantly higher levels of all 4 synaptic markers compared to the Tg:PBS, Tg:FUS, and Tg:mAb mice ($p < 0.01$), while there was no significant difference in these levels between the Tg:mAb + FUS animals and the WT groups (Fig. 4c, d). These results indicate that synapse loss was at least partially spared by the FUS-mAb combination treatment in aged APP/PS1dE9 mice. This result is in line with our cognitive data and suggests a pro-cognitive health phenotype in the APP/PS1dE9 mice that received the mAb and FUS-BBBD.

2.7. Altered plaque-associated microglia and macrophage activation in aged APP/PS1dE9 after treatment with 07/2a and FUS-BBBD

Amyloid plaques are often surrounded and infiltrated by immune cells, such as microglia and astrocytes, in AD brain. Thus, we investigated the morphology and colocalization of these cells with plaques in mouse brain by immunostaining for Iba-1 and CD68 (markers for microglia and macrophages) and GFAP (an astrocyte marker). Immunoreactivities of Iba-1 were significantly increased in hippocampal CA3 of the Tg:mAb and Tg:mAb + FUS mice compared to animals in the Tg:PBS group ($p < 0.05$), while no significant difference was found between groups in the pre-frontal cortex (Fig. 5a-c). The Tg:mAb and Tg:mAb + FUS mice had more activated microglia/macrophages associated with Aβ plaque in the hippocampus, as indicated by increased Iba-1 fluorescent intensity ($p < 0.05$, Fig. 5d, e); this result is consistent with reactive microgliosis. In addition, CD68 fluorescent intensity associated with Aβ, indicative of lysosomal phagosomes, was significantly increased over the Tg:PBS animals only in the Tg:mAb group ($p < 0.05$), while no difference was observed in the Tg:mAb + FUS mice (Fig. 5d-f). This result suggests that the pGlu-Aβ mAb, but not FUS-BBBD, induced phagocytosis of Aβ plaques *via* increased microglia activation or through macrophages. GFAP-positive astrocytes were clustered around Aβ plaques in the hippocampus of the APP/PS1dE9 mice, but no treatment-related effects were observed in either the hippocampus or pre-frontal cortex treatment with the anti-pGlu3 Aβ mAb alone or in combination with FUS-BBBD (Fig. 6a, b).

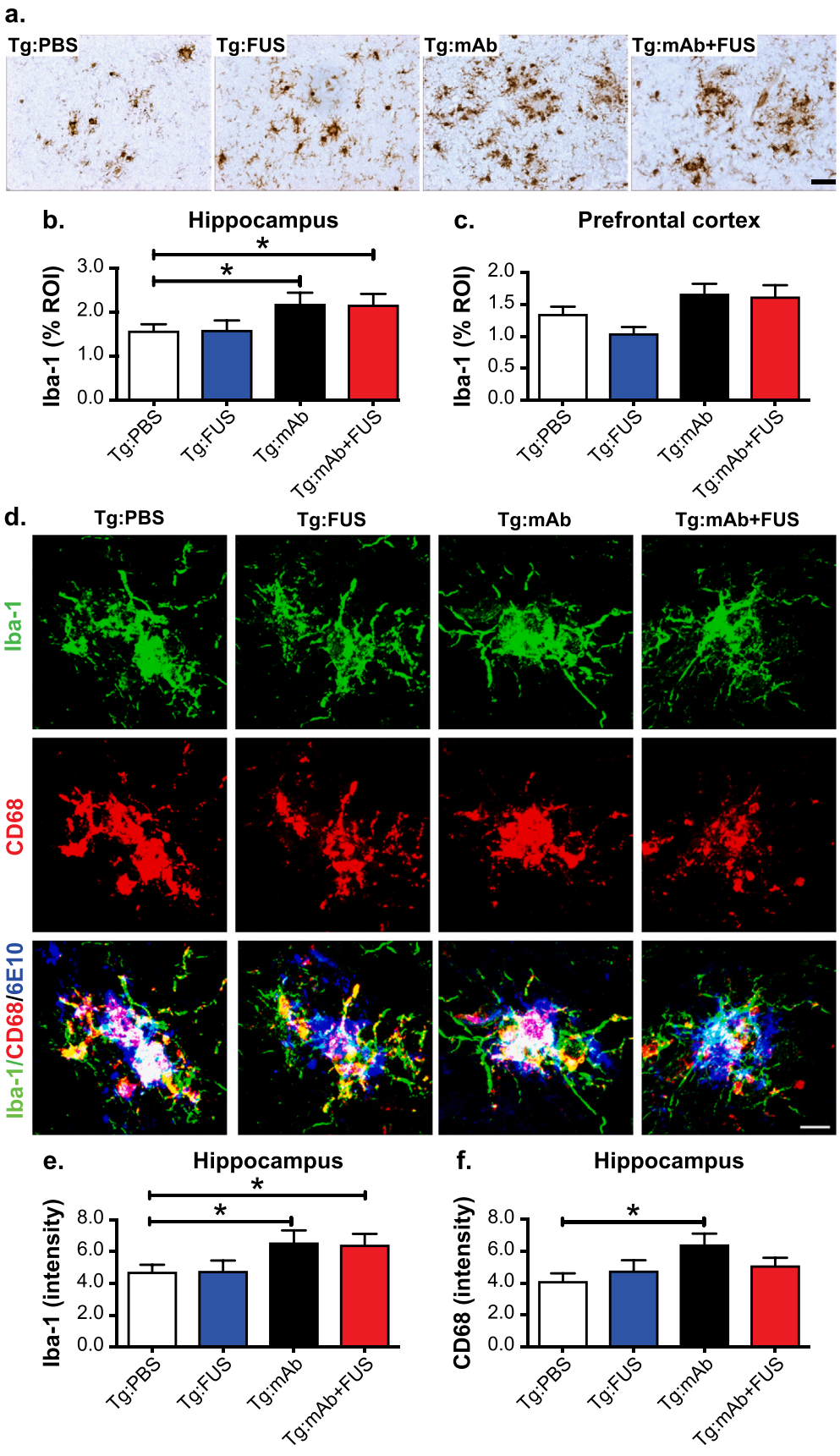

Fig. 5. Morphological changes and glial phagocytosis in WT and Tg mice treated with or without FUS-BBBD and pGlu3 Aβ mAb 07/2a. a-c. Iba-1-positive immunostaining (a) showed significant increased activation of microglia and macrophages (i.e. rounder cell bodies and thickened processes) and the clustering of more Iba-1-positive glial cells in sonicated hippocampal CA3 region in the Tg:mAb and Tg:mAb + FUS mice compared to the Tg:PBS group (b) (*$p < 0.05$, 3 equidistant planes 300 μm apart). Iba-1 positive immunostaining was not significantly different in the non-sonicated prefrontal cortex between groups. Scale bar = 50 μm. d-f. High-resolution confocal images of microglia/macrophages (immunoreactive for Iba-1) and phagocytic cells (immunoreactive for CD68) in the hippocampal CA3 region (d), Scale bar = 25 μm. Quantification of immunofluorescence intensity indicated increased microglial acitivation (Iba-1 immunofluorescent intensity) in the Tg:mAb and Tg:mAb + FUS mice, and increased phagocytosis (CD68 immunofluorescent intensity) in Tg:mAb animals (*$p < 0.05$, compared to Tg:PBS group). (Tg:PBS, n = 9; Tg:FUS, n = 7; Tg:mAb, n = 9; Tg:mAb + FUS, n = 6; one-way ANOVA followed by Tukey's post-hoc test; (*$p < 0.05$).

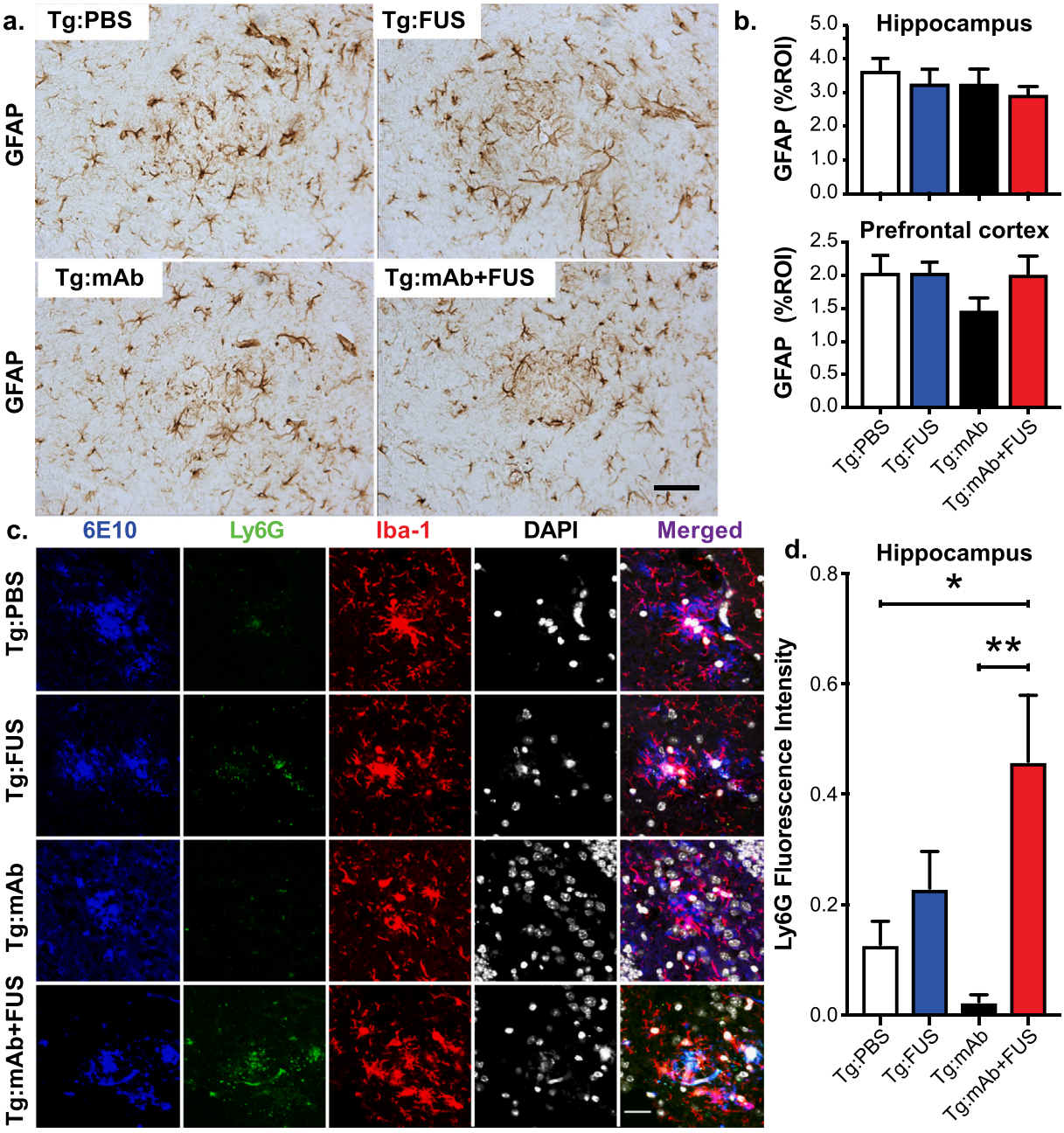

Fig. 6. Plaque-associated astroglia and monocytes. a-b. Astrocytic immunoreactivity of GFAP in hippocampus and PFC in mice from the Tg:PBS, Tg:FUS, Tg:mAb and Tg:mAb + FUS groups. No significant differences in GFAP immunoreactivity were found between different groups. Scale bar = 50 μm. c-d. Confocal microscopy of Ly6G, Iba-1, DAPI, and 6E10 immunofluorescence in hippocampal CA3 of Tg mice with or without FUS-BBBD and pGlu3 Aβ mAb. Scale bar = 25 μm. Fluorescence intensity of Ly6G (b) was significantly higher in the Tg:mAb + FUS group compared to the Tg:PBS and Tg:mAb groups. (Tg:PBS, n = 9; Tg:FUS, n = 7; Tg:mAb, n = 9; Tg:mAb + FUS, n = 6; one-way ANOVA followed by Tukey's post-hoc test; (*$p < 0.05$, **$p < 0.01$).

2.8. Increased Ly6G-positive plaque-associated immune cells in APP/PS1dE9 mice after treatment with 07/2a and FUS-BBBD

Ablation or inhibition of monocyte migration into the brain has been shown to exacerbate Aβ pathology, while enriching monocytes in blood and enhancing their recruitment to plaque lesion sites greatly diminishes Aβ plaque load in AD Tg mice [29]. The immunofluorescent intensity of the lymphocyte antigen 6 complex locus G6D (Ly6G), a marker for infiltrating monocytes, showed a significant increase of Ly6G cells associated with Aβ plaques in the Tg:mAb + FUS animals compared to those in the Tg:PBS and Tg:mAb groups ($p < 0.05$, $p < 0.01$, Fig. 6c, d). No significant difference in Ly6G immunofluorescence was found between the Tg:mAb and Tg:PBS groups or between the Tg:FUS group and all other groups. These data suggest that FUS-BBBD in combination with the anti-pGlu3 Aβ mAb facilitated monocyte infiltration into the brain and within the vicinity of the Aβ plaques, which may have contributed to plaque clearance in the mice given the combination treatment.

2.9. FUS-BBBD did not increase microhemorrhages or reduce neuron number

We used hemosiderin staining to investigate the presence of microhemorrhages, which are infrequent in APP/PS1dE9 mice at 17 months of

age. We found FUS-BBBD with or without 07/2a administration did not increase the number of microbleeds in the brain (Fig. 7a, b). These results indicate that the cavitation monitoring and control was successful in ensuring that the FUS treatments did not induce vascular damage or associated damage of the brain parenchyma, nor did it enhance the number of hemosiderin-positive microhemorrhages. In addition, we observed no differences between groups in the number of neurons in hippocampal layers CA1 and CA3, indicating that FUS-BBBD treatment did not affect neurons (Fig. 7c, d).

3. Discussion

Our results revealed that the effects of the anti-pGlu3 Aβ 07/2a mAb in aged APP/PS1dE9 mice are improved when combined with MB-enhanced FUS-BBBD, leading to improved learning ability, slowing of cognitive decline, and preserved synapses in the hippocampus, possibly by engaging microglia and monocytes, thereby promoting clearance of Aβ and reducing the plaque load. We previously showed that weekly intraperitoneal (i.p.) injections of 07/2a in plaque-rich 12-month-old APP/PS1dE9 mice for 16 weeks lowered plaque burden and improved spatial learning and memory in the Water T Maze [22]. It is possible that increasing delivery of the mAb with FUS-BBBD led to an improved antibody treatment effect. It is also possible that effects of the BBBD itself contributed to the improvements, as others have demonstrated that FUS-BBBD alone can increase Aβ clearance in AD model mice, presumably by microglia activation [14,16]. While more work is needed to elucidate the relative importance of enhancing delivery and the effects of FUS-BBBD itself, these results indicate that the combination could be used to enhance the effects of this mAb and may provide additional efficacy by facilitating the infiltration of peripheral monocytes to clear Aβ. These results are exciting, as an anti-pGlu3 Aβ mAb is showing promising results in early clinical trials [30].

Our findings that combination of these two treatments over 3 weeks in aged APP/PS1dE9 mice exerts additive effects compared to either treatment alone is in agreement with other work demonstrating that FUS enhances the CNS uptake of peripherally administered antibodies [12,14] or other therapeutics [13,31] targeting AD pathology. This work is also in agreement with prior studies in AD model mice [17] and in dogs [32] in that MB-enhanced FUS did not result in increased microhemorrhages or other associated irreversible effects, even in aged animals with significant disease.

Our findings do not align with previous reports that FUS-BBBD alone can markedly ameliorate the pathology of Aβ-deposition and behavior. Burgess et al. found a 19% reduction in plaque number after three

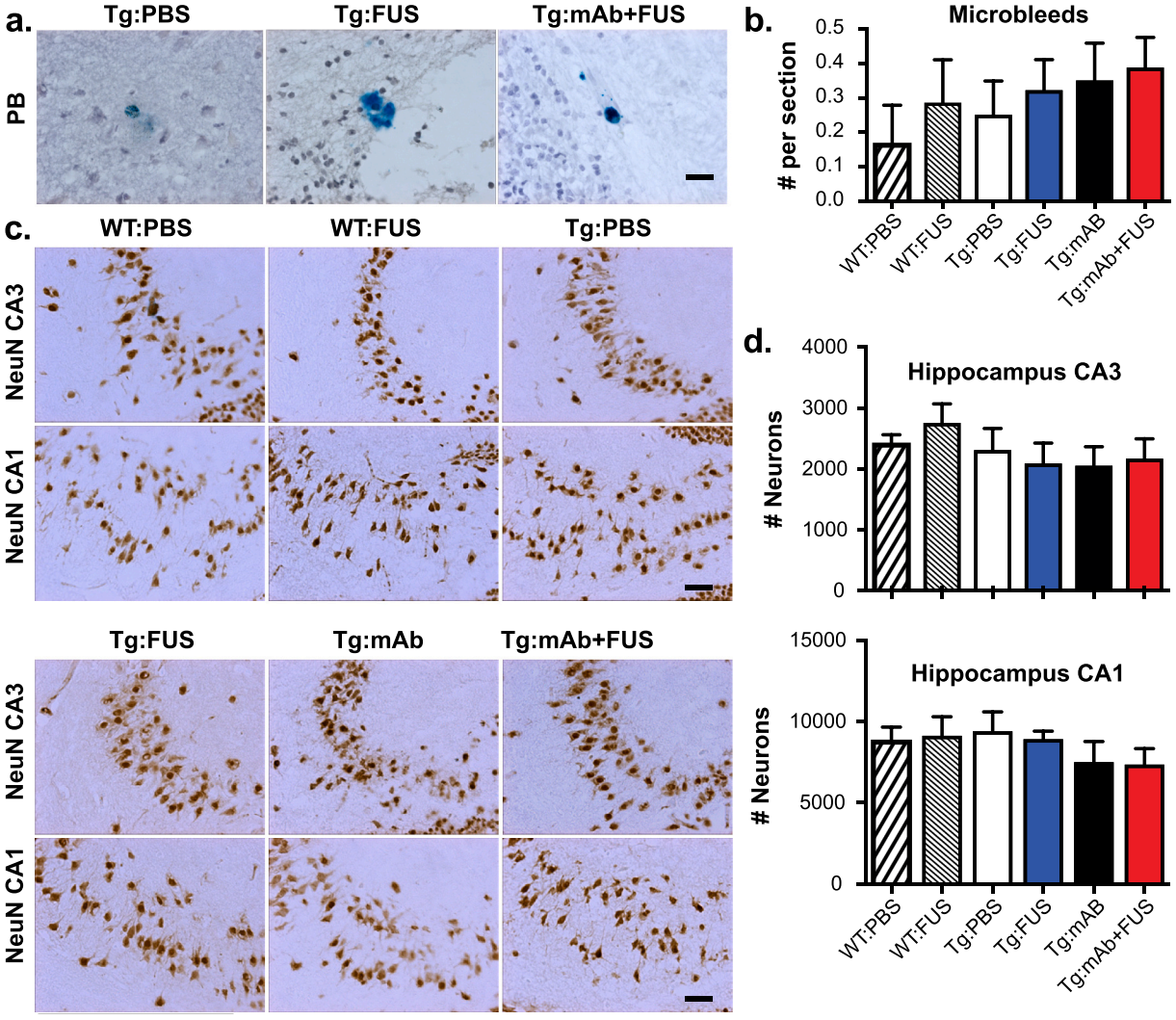

Fig. 7. Microhemorrhage and neuron numbers in WT and Tg mice with or without FUS-BBBD and pGlu3-Aβ mAb. a-b. Hemosiderin staining. No significant difference in microhemorrhage number was found between the different groups. Scale bar = 25 μm. c-d. Stereology of NeuN-positive cells (indicating neurons) in hippocampal CA3 and CA1. Scale bar = 50 μm. No significant difference in neuron number was found between the different groups. (WT:PBS, n = 13; WT:FUS, n = 8; Tg:PBS, n = 9; Tg:FUS, n = 7; Tg:mAb, n = 9; Tg:mAb + FUS, n = 6; one-way ANOVA followed by Tukey's post-hoc test).

weekly sessions of FUS-BBBD in 7 month-old TgCRND8 mice [15]. Leinenga and Götz found over 50% reductions in both plaque number and area in 12–13 month-old APP23 mice after five scanning FUS-BBBD sessions [16]. However, in a subsequent study, that group did not see a reduction in plaque area in 21–22 month-old APP23 mice after four scanning sessions, although they did see changes in plaque size and increased numbers of Iba-1-positive cells [17]. Here, in 17.5-month-old APP/PS1dE9 mice, we did not find significant reductions in plaque burden or improvement in learning in the Water T Maze test with three weekly sessions of FUS-BBBD alone. These results suggest that treatment with FUS-BBBD alone might be less effective in older mice. However, differences in mouse model disease state (independent of age), FUS procedure, and other methodologies could confound direct comparison between studies. We did not observe any transgenic or treatment effects on anxiety-related behaviors however. Reports of anxiety-like behavior in APP-PS1 mice are inconsistent, with studies showing increased, decreased, and no change in anxiety in the Open Field and Elevated Plus Maze tests [33].Other studies have shown that freezing in the conditioning context in the Contextual Fear Conditioning test was reduced in APP-PS1 mice, but not statistically different from WT mice (8 and 13 months of age) [34]. This is a similar finding to what we observed in the present study. Many factors such as experimental design (number of shocks, use of a tone), genetic background (B6 v. B6C3), sex, and previous experience of the mice can account for differences in phenotypic outcomes in APP/PS1 mice. Experiments with increased numbers of subjects might also detect small improvements after FUS-BBBD that our study was underpowered to detect.

Prior work from our lab and others have demonstrated the efficacy of anti-pGlu3 Aβ antibodies in Alzheimer's-like Tg mouse models. We reported that chronic treatment starting before and after Aβ deposition resulted significant lowering of pGlu3 Aβ and total Aβ deposits without inducing microhemorrhages in APP/PS1dE9 mice [20–22]. Our current results differ slightly from our previous work [22] in that we did not see a reduction of pGlu3 Aβ plaque deposition in prefrontal cortex following the combination treatment in aged APP/PS1dE9 mice. This is likely due to the fact that the mice in this study were immunized only 3 times, compared to 16 times in the previous study, and the plaque-lowering was better in the sonicated hippocampal region, as expected. Another study in PDAPP mice demonstrated that a different pGlu3 Aβ specific mAb (mE8-IgG2a; Eli Lilly) reduced amyloid burden in the absence of microhemorrhages [35]. Our lab has also investigated the effects of anti-pGlu3 Aβ antibodies on cognitive decline in APP/PS1dE9 Tg mice and reported a significant sparing of spatial learning and memory in the Water T Maze following treatment [19,22].

Currently, a humanized anti-pGlu3 Aβ antibody, Donanemab (LY3002813; Eli Lilly and Co.), is being tested in early-stage AD patients in clinical trials. The initial results of two small Phase 1 studies, presented at the Alzheimer's Association International Conference (AAIC, 2016) and Clinical Trials in Alzheimer's Disease (CTAD, 2019), showed that patients who received a high dose (10–20 mg/kg) of Donanemab by monthly intravenous injections had significant plaque removal in the brain by amyloid PET imaging. ARIA with Hemorrhage (ARIA-H) were apparent in 2 participants in one trial while the incidence of ARIA-E (ARIA with Edema), an adverse event associated with amyloid immunotherapy [36], was observed in 1 of every 4 participants in the second Phase 1 trial (www.alzforum.org). While Donanemab was shown to effectively reduce plaques, it induced an anti-drug antibody response in many participants, thereby reducing the antibody's half-life in the circulation [37,38]. More recently, Eli Lilly initiated two larger Phase 2 studies of Donanemab (TRAILBLAZER-ALZ and TRAILBLAZER-ALZ2) in early AD with a primary focus on cognitive and functional outcomes. Eli Lilly presented a press release in mid-January 2021 describing a positive outcome for the TRAILBLAZER-ALZ trial: robust lowering of cerebral amyloid and significant 33% slowing of cognitive and functional decline in patients receiving Donanemab [30]. Our current study suggests that the success of pGlu3 Aβ immunotherapy can be improved with FUS-BBBD, possibly with lower antibody dosing and without increasing risk for microbleeds.

FUS-BBBD and anti-Aβ immunotherapy appear to alter the microenvironment in potentially beneficial ways. Microglia activation and the phagocytosis of Aβ has been observed in anti-Aβ immunotherapy, presumably *via* microglial Fcγ-receptor binding to antibody-opsonized Aβ aggregates [39]. Our data suggest that anti-pGlu3 Aβ mAb (07/2a) treatment increased the recruitment of microglia to plaques, resulting in increased phagocytosis of Aβ. In addition, infiltrating monocytes were increased in hippocampus 3 weeks after the last combined mAb and FUS-BBBD treatment, which appears to have had a beneficial, plaque-clearing effect in this short-term study. Depletion of monocytes or inhibition of monocyte migration into the brain has been shown to worsen Aβ pathology, while enriching monocytes in blood and enhancing their recruitment to plaque lesion sites greatly diminishes Aβ plaque load in AD Tg mice [29]. It is possible that FUS-BBBD locally modulates activity and migration of microglia and monocytes, accelerating antibody-mediated Aβ clearance in aged AD Tg mice through increasing cerebral recruitment of monocytes overexpressing Aβ-degrading enzymes, as well as increase peripheral monocyte-derived macrophages. In line with this, it was recently reported that MR-guided FUS-BBBD led to an immediate and transient influx of neutrophils, a peripheral leukocyte, in another AD Tg mouse model [40].

These changes to the brain we observed after the combined 07/2a + FUS-BBBD treatment may also protect synapses. Consistent with earlier work, we observed plaque-associated hippocampal synaptic degeneration in the aged APP/PS1dE9 mice [41]. However, mice in the Tg:mAb + FUS group had less synapse loss along with a decreased plaque burden. Microglia have been shown to be highly phagocytic and participate in synapse elimination during aging and AD [28,42]. Perhaps FUS-BBBD facilitates monocyte infiltration and lowers microglia overactivation, thereby reducing microglial synapse phagocytosis and modulating the glial response to pGlu3 Aβ. It is also possible that other cells or molecules, such as growth factors, entered the brain from the periphery during FUS treatment and had independent effects on synapses and memory. Further studies are underway to address this mechanistic question.

In conclusion, three weekly sessions of MB-enhanced FUS BBBD in the hippocampus improved the effects of an anti-pGlu3 Aβ mAb, selectively reducing plaque burden and synapse loss in the targeted area and improving spatial memory more quickly and in a greater percentage of animals. The combined procedure did not increase the incidence of microhemorrhage in the context of CAA in aged AD Tg mice with both plaque and vascular amyloid deposition. Interestingly, our data suggests adding FUS-BBBD can ameliorate pathology and neuroinflammation by modulating the activation and infiltration of phagocytes. Therefore, our study highlights the potential of using this technique to improve the brain delivery and thereby, the efficacy of the anti-pGlu3 Aβ mAb.

4. Materials and methods

4.1. Animals

C57BL/6 J and APPswe/PS1dE9 breeder mice were obtained from The Jackson Laboratory and bred in-house for this study. Mice were genotyped by PCR using the following primers: APP/PS1dE9: 5′-GACTGACCACTC GACCAGCTT-3′ and 5'-CTTGTAAGTTGGATTCTCATAT-3′. Mice were aged to 24–30 months for a single dose study to determine the antibody concentration in brain tissue with and without FUS-BBBD, and 16 months for a three dose FUS-BBBD study. Only males were used for this study to reduce gender-specific variability in the behavioral tests. At the end of each study, mice were anesthetized, blood collected, and the brain perfused with saline prior to harvest.

All animal studies were approved by the Institutional Animal Care and Use Committees at Harvard Medical School and Brigham and Women's Hospital. The Harvard Medical School and Brigham and

Women's Hospital animal care and management programs are accredited by the Association for the Assessment and Accreditation of Laboratory Animal Care, International (AAALAC) and meet the National Institutes of Health standards as set forth in the 8th edition of the Guide for the Care and Use of Laboratory Animals. The institutions also accept as mandatory the PHS Policy on Humane Care and Use of Laboratory Animals by Awardee Institutions and NIH Principals for the Utilization and Care of Vertebrate Animals Used in Testing Research and Training. There is an approved Assurance of Compliance (A3431–01 for Harvard Medical School and A4752–01 for Brigham and Women's Hospital) on file with the Office of Laboratory Animal Welfare (OLAW).

Animals were anesthetized by i.p. injections of ketamine (80 ml/kg/h) and xylazine (10 ml/kg/h) or isoflurane before FUS-BBBD or administration of mAb or PBS. Isoflurane was applied through a nosecone with medical air as the carrier gas. The isoflurane concentration was titrated based on the respiration rate and was typically 1–2%. A catheter was placed in the tail vein for i.v. administration.

4.2. Antibody, FUS-BBBD, and/or PBS treatment

A total of 52 male mice were utilized in the 3-dose study (~23–35 g). Sixteen month-old mice were divided into 6 groups and received one of the following treatments: WT:PBS, 130 μl sterile PBS i.v. in WT mice (n = 13); WT:FUS, FUS-BBBD in WT mice (n = 8); Tg:PBS, 130 μl sterile PBS i.v. in APP/PS1dE9 mice (n = 9); Tg:FUS, FUS-BBBD in APP/PS1dE9 mice (n = 7); Tg:mAb, 500 μg anti-pGlu3 Aβ 07/2a mouse mAb (divided into 4 consecutive infusions of 13 μl each containing 125 μg mAb) generated and provided by Vivoryon Therapeutics AG (Halle, Germany), i.v. in APP/PS1dE9 mice (n = 9); Tg:mAb + FUS, 500 μg anti-pGlu3 Aβ 07/2a mouse mAb (13 μl × 4) immediately prior to FUS-BBBD in APP/PS1dE9 mice (n = 6). Mice were treated with a total volume of 130 μl liquid (antibody and/or PBS and/or MB) to limit the volume of liquid to what the mouse can tolerate. Behavior tests were initiated one week after the third and final treatment. The wildtype animals were included to compare with the Tg mice in the behavioral tests and to study whether the FUS-BBBD procedure caused behavioral changes or brain tissue damage. Thus, we did not treat wildtype mice with 07/2a mAb. The experiments were performed in three cohorts with animals from each group present in each cohort.

4.3. FUS-BBBD

Before the ultrasound exposures, the scalp was shaved and remaining fur on the head was removed using depilatory cream to ensure unimpeded ultrasound propagation. A catheter was placed in the tail vein, and the animal's head was fixed in a plastic stereotactic frame that was built in-house. This frame was placed on the FUS device. Sonications (10-ms bursts applied at 2 Hz for 100 s) were applied concurrently with an injection of the MB ultrasound contrast agent Optison (GE Healthcare, Little Chalfont, Buckinghamshire, UK; dose: 100 μl/kg; diluted 4× in PBS) to open the BBB. Two locations in each hemisphere were sonicated in each session (± 2 mm lateral, 3 mm dorsal, and 2 and 3.5 mm anterior to the interaural line). The time between sonications was at least two minutes to allow for the MB to mostly clear from circulation.

A FUS system with cavitation-controlled transmission was designed and built in-house [43]. An air-backed, spherically curved transducer (diameter/radius of curvature: 10/8 cm) was used for FUS transmission with a resonant frequency of 278 kHz. The transducer was attached to a three-axis positioning system (A4000, Velmex, Bloomfield, NY, USA) (Fig. 1a). The transcranial sonications were applied at the third harmonic of the FUS transducer (835 kHz) *via* a function generator (33220A, Agilent, Santa Clara, CA, USA) and an amplifier (240 L, E&I, Rochester, NY, USA). The electrical power was measured using a power meter (E4419B, Agilent, Santa Clara, CA, USA) and dual-directional coupler (C5948–10, Werlatone, Patterson, NY, USA); a radiation force balance was used to measure the transducer efficiency. The pressure field in the focal plane was mapped using a needle hydrophone (HNC-1000; Onda, Sunnyvale, CA). This map, along with radiation force balance measurements, was used to estimate the pressure amplitude at the focus in water. The half-width and -length of the 50% isopressure contours were 1.9 and 11.4 mm respectively. The pressure amplitude used in the mouse sonications was 0.33 MPa (estimate in water).

Acoustic emissions were monitored using a 10-element piezoelectric hydrophone. The elements of this passive cavitation detector were arranged in a ring (inner/outer diameter: 13/15 cm) that surrounded the transducer. The cavitation emission signals were recorded with a 12-bit high-speed digitizing card (PCX-5124, National Instruments, Austin, TX, USA). Frequency spectra were generated *via* fast Fourier transform, and the harmonic and wideband emissions were tracked in real time using software developed in-house [43] in MATLAB (MathWorks, Natick, MA, USA). The software acquired baseline emissions prior microbubble injections and then waited for the user to administer microbubbles. Once the injection started, harmonic (2×, 3×, 4× 835 kHz) and wideband emissions were calculated in dB relative to baseline emissions. This cavitation-controlled system was used to confirm that stable cavitation was occurring (detected by harmonic emission), as well as to avoid inertial cavitation (assessed by wideband emission). If wideband emission was detected in the cavitation controller, the exposure level was automatically decreased.

To validate this system, a pilot study was performed in WT mice that visualized the BBB opening by obtaining fluorescence imaging of the delivery of Trypan blue after sonication. The images were obtained with a system developed in-house consisting of two red LED lamps (610–630 nm, GR-PAR38-12 W-R-1, ABI, Indianapolis, IN) for excitation, and a bandpass filter (687–748 nm, 715AF58, Omega Optical, Brattleboro, VT, USA) and digital camera (C920, Logitech) for image acquisition.

4.4. ELISA - Measuring anti-pGlu3-Abeta 07/2a mAb in the soluble fraction of mouse brain homogenates

In order to determine whether FUS-BBBD affected antibody delivery to the brain, we injected 300 μg of the anti-pGlu3 Aβ mAb 07/2a i.v. with or without FUS-BBB disruption in the hippocampus in the left hemisphere in 10 male APP/PS1dE9 mice (24–30 months of age) and measured the mAb concentration in the brain by ELISA 72 h later. To prepare the brain for anti-pGlu3-Abeta 07/2a mAb-ELISA analysis, the left hemisphere was homogenized in TBS buffer (Thermo Fisher Scientific) at a concentration of 150 mg brain per ml buffer containing protease inhibitor cocktail (Complete mini, Roche) and 0.1 mM AEBSF by using a Precellys homogenizer (VWR). The homogenate was centrifuged for 30 min at 25.000 × g, supernatants were collected thereby yielding the soluble TBS fractions. The protein concentration in the TBS fraction was determined using BCA Protein Assay Kit (Thermo Fisher Scientific). To quantify 07/2a antibody concentrations in brain homogenates, streptavidin coated 96-well plates were blocked with Pierce™ Protein-Free blocking buffer for 2 h at RT and further treated with 20 ng of biotinylated pGlu3-Aβ3–17 peptide in each well at 4 °C for 2 h. After washing, antibody standards and brain samples were added to the plate and incubated at 4 °C for 2 h. The plates were washed three times and then incubated with anti-mouse IgG-HRP 500 ng/ml at 4 °C for 1 h. For detection, 100 μl SureBlue™ TMB substrate solution (KPL) were added to each well for 30 min at RT and then the reaction stopped by adding 50 μl of 1.2 N H2SO4. A SUNRISE Microplate Reader (Tecan) was used to measure optical density values at the wavelength of 450 nm. The quantification was normalized to the corresponding brain weight of each sample in TBS fraction, respectively.

4.5. Behavior tests (performed in the following order)

4.5.1. Open Field Test (OF)

The OF test was performed as previously described [44] to assess general locomotor behavior in a novel environment. Briefly, mice were

allowed free exploration in an open field chamber made of clear Plexiglass (27.31 × 27.31 × 20.32 cm) (Med Associates) for one hour. A computer-assisted infrared tracking system and software (Activity Monitor; Med Associates) was used to record the number of beam breaks. Total distance traveled (cm) in 5 min time bins was used as a measure of general locomotor activity.

4.5.2. Water T Maze Test (WTM)

The WTM is a test of spatial learning and memory in which mice learn to use the spatial cues in a room to navigate to a hidden platform to escape from the water. Testing was performed as previously reported [44]. The testing apparatus is a plus maze made of clear Plexiglass with each arm designated as N, S, E, or W. The maze was filled with water and an escape platform was placed on the E side of the maze submerged approximately 1 cm below the surface of the water. A divider was placed on the maze to block off the appropriate arm so that the mouse could choose only the E or W arm for escape. Mice were given 10 trials each day with semi-randomized starting points from the N and S positions. Learning was assessed by two measures, 1) the percent of correct responses out of 10 trials across 8 training days and 2) the number of days to reach a criterion. The criterion was defined as a score of 80% or more correct responses for 2 consecutive days. The 80% criterion is a common, well-accepted convention across many learning and memory studies [45–47]. We have used this 80% criterion across multiple Water T Maze studies and found that it is a reliable indicator of stable performance. When a mouse reaches 80% across two consecutive days, the performance of the mouse typically remains stable throughout the remainder of the testing period. If a mouse did not reach this criterion, it was assigned a number based on its score on day 8. If the mouse scored 80% or better on day 8, it was assigned a 9. If a mouse scored less than 80% on day 8, it was assigned a 10.

4.5.3. Contextual Fear Conditioning Test (CFC)

Contextual Fear Conditioning was used to assess fear learning and memory as previously reported [44]. Mice show a fear response (freezing) when exposed to brief, aversive foot shock stimuli during training and when re-exposed to the context where the mouse received the foot shock. During training, mice were exposed to the fear conditioning chambers (Med Associates) for 2 min, were given two foot shocks (0.5 mA; 2 s) separated by 2 min, and were removed from the chamber 1 min after the last foot shock. The context test, which assesses memory for the place where the mice received the foot shock, was performed approximately 24 h after training. During the context test, mice were placed back into the conditioning chamber with no electric shock, and freezing was measured for 3 min. The freezing response (Topscan software Cleversys) was used as a surrogate marker of memory performance as mice that remember receiving the shock during the training phase on day 1 are expected to spend a significant amount of time freezing during the context test on day 2.

4.6. Pathological and biochemical analyses

4.6.1. Immunohistochemistry

Mouse hemibrains were fixed in 4% PFA for 24 h, cut into 10 μm cryosections, mounted onto microscope slides, and immunostained as previously described [44]. Brain sections were incubated with anti-Aβx-42 (1:200, Covance), anti-Aβ 6E10 (1:1000, Covance), anti-pGlu3 IgG2b (1 μg/ml; Vivoryon Therapeutics) and NeuN (1:200, Serotec) mouse monoclonal antibodies, or Aβ40 (1:200, Covance), Iba-1 (1:200, Wako) and GFAP (1:1000, DAKO) rabbit polyclonal antibodies, DAPI or CD68 (1:250, Serotec) rat polyclonal antibody overnight at 4 °C. Sections were washed in TBS and then incubated with biotinylated secondary antibodies and developed using Vector ELITE ABC kits (Vector Laboratories) and 3,3-diaminobenzidine (Sigma-Aldrich) or immunofluorescent-labeled secondary antibodies and cover-slipped with mounting media (Vector).

4.6.2. Aβ load analysis

Aβ immunoreactivity for all mice was captured by imaging sections in a single session under a Nikon Eclipse E400 microscope. Aβ plaque load and Aβ plaque size were quantified within a region of interest (ROI) using the Bioquant image analysis system (Nashville, TN). Three sections at equidistant planes were analyzed per mouse by an operator who was blinded to mouse genotype and treatment.

4.6.3. Aβ ELISAs

Tper-insoluble, guanidine hydrochloride-extracted brain homogenates were extracted from mouse hemibrain, including cortex and hippocampus, and run on an MSD Aβ Triplex ELISA as previously described [44].

4.6.4. Confocal analysis of glia morphology and association with Aβ plaques

Immunofluorescence for Aβ plaques (6E10), microglia/macrophages (Iba-1) and (CD68) was detected by confocal microscopy (Zeiss, LSM 710; Carl Zeiss). Images were collected using the same exposure settings. Confocal *Z*-stack images (optical slices of 0.2 μm) of plaques and surrounding glia were collected using a 63× objective. Three images were acquired from 3 equidistant planes, 500 μm apart per mouse. Immunofluorescent intensity analysis and 3D reconstruction of Z-stack images were performed with confocal image analysis software, Zein black (Carl Zeiss). Glia counts were performed using stereological methods after collecting images.

4.6.5. Synaptic puncta staining and analysis

Immunofluorescent staining of pre- and post-synaptic markers and analyses were performed as previously described [44,48]. Fixed, frozen brain sections were dried, washed in Tris-buffered saline (TBS), and blocked with 20% goat serum +0.3% Triton X-100 in TBS for 2 h. Primary antibodies were diluted in antibody buffer with 0.03% Triton X-100 and 10% goat serum as follows: Vglut2 (Millipore goat anti-guinea pig, 1:1000), Homer1 (R&D Systems goat anti-mouse, 1:200), GluR1 (Abcam goat anti-rabbit, 1:200), and SYN-1 (Millipore goat anti-rabbit, 1:200) and incubated overnight at 4 °C. Secondary Alexa Fluor-conjugated antibodies (Life Technologies) were added at 1:200 in 0.03% Triton X-100 with 10% goat serum for 2 h at room temperature (RT). Confocal imaging was performed using a ZEISS LSM710 confocal microscope and a 63× oil objective. Images were acquired using a 1 Airy Unit (AU) pinhole, while holding the gain and offset parameters constant for all sections and mice for each experiment.

4.6.6. Preparation of synaptosome fractions

Hippocampal synaptosome fractions were prepared as described previously [44,49]. Hippocampi were dissected and homogenized in a glass mortar using a rotating Teflon pestle (2000 rpm) for about 20 passes to generate a Dounce homogenate that was centrifuged at 1000 x*g* for 10 min to remove nuclei and debris (first pellet: P1). The supernatant (S1) was centrifuged at 10,000 x*g* for 15 min to acquire the second pellet (P2) and supernatant (S2) was collected (i.e. cytosolic fraction). The P2 pellet underwent detergent extraction by adding 8 volumes of Triton X-100 buffer (final = 0.5% *v*/v) containing 10 mM Tris, pH 7.4, 1 mM Na_3VO_4, 5 mM NaF, 1 mM EDTA and 1 mM EGTA, and was then rocked gently at 4 °C for 20 min to form the synaptosome fraction.

4.6.7. Western blotting of synapse markers

Western blotting was performed on hippocampal synaptosomes as previously described [28,44] using rabbit polyclonal antibody Synapsin-1 (SYN-1, 1:200; Millipore), goat anti-guinea pig antibody VGlu2 (1:1000; Millipore), goat anti-rabbit antibody GluR1 (1:200; Abcam) and mouse mAb PSD95 (1:200; Millipore), and GAPDH (1:200; Millipore). Protein concentrations were determined using the BCA assay. Twenty micrograms of total protein were loaded into each lane, separated by 4%–12% SDS-PAGE, followed by transfer to a nitrocellulose

membrane. Blots were blocked for 1 h at RT and then incubated in primary antibody overnight at 4 °C. The next day, the membranes were rinsed and incubated for 1 h with fluorescent-tagged goat anti-rabbit or anti-mouse IgG (1:5000; Life Technologies). Blots were scanned using a LiCor Odyssey Infrared Imaging System. Intensity of bands was measured by LiCor Odyssey software.

4.6.8. Stereological quantification of neurons

Immunohistochemistry for anti-neuronal nuclear protein, NeuN (1:250; Millipore Bioscience Research Reagents) was performed as described previously [50]. Stereological counting of neurons was performed on 10 μm sagittal, immunostained sections at each of 6 planes 250 μm apart per mouse using the optical dissector method. Cells were counted in an area of ~300 μm within a 10 μm depth per brain region examined. The number of neurons per section in each brain region was estimated using ~15 optical dissectors and the Bioquant image analysis system according to the principles of Cavalieri [51].

4.6.9. Quantification of microhemorrhages

Microhemorrhages were visualized by staining brain sections with hemosiderin (2% potassium ferrocyanide in 2% hydrochloric acid). Microhemorrhages were quantified by counting hemosiderin-positive foci over the entire sagittal section for each of 2 adjacent sections at 3 equidistant planes approximately 250 μm apart per mouse. Slide labels were covered and renumbered to blind the scorer to the animal treatment group. The number of hemosiderin-positive foci was averaged for each mouse.

4.7. Statistics

4.7.1. Statistical analysis

Data are expressed as mean ± SEM. When more than two groups were compared, data were analyzed using one-way ANOVA followed by Tukey's honest significant difference post-hoc (HSD) test. Analysis of the WTM test over 8 days was made using repeated measures ANOVA followed by Tukey's HSD post-hoc test. When only two groups were compared, we used unpaired, two-tailed *t*-tests. Behavioral test analysis was performed using StatView Version 5.0 software; all other data were analyzed using Prism Version 6.0 (GraphPad) software. A p value of <0.05 was considered significant.

Funding

This work was funded by grants from The Focused Ultrasound Foundation (Charlottesville, VA) to CAL and NJM, the National Institutes of Health, NIH/NIA R01 AG040092 and NIH/NIA RF1 AG058657 to CAL, and NIH/NIBIB R01 EB028686 to NJM.

Availability of data and materials

The datasets generated and/or analyzed during the current study are available from the corresponding authors upon reasonable request.

Declaration of Competing Interest

We declare that Stephan Schilling is a former and Thore Hettmann, present, employees of Vivoryon Therapeutics N.V., Germany, and hold stock options of the company. Stephan Schilling is an advisor to Vivoryon Therapeutics N.V. Co-senior author, Cynthia A. Lemere, was an unpaid scientific advisory board member for Vivoryon Therapeutics N.V., receives antibodies, and has previously received unrestricted funding from Vivoryon Therapeutics N.V. for some of her past work on pGlu3 Aβ immunotherapy. She serves as a consultant to Biogen and Acumen Pharmaceuticals, both of which are developing anti-amyloid immunotherapies, and Apellis Pharmaceuticals. Brigham and Women's Hospital holds two patents related to this work.

Acknowledgements

The authors thank Grace Liu (BWH Neurology) for her assistance with mouse breeding and P. Jason White and Can Barış Top (BWH Radiology) for their assistance with the experiments. We thank Jens-Ulrich Rahfeld for critical comments on the manuscript. Vivoryon Therapeutics is thanked for providing the 07/2a mAb as a gift-in-kind.

References

[1] J. Hardy, D.J. Selkoe, The amyloid hypothesis of Alzheimer's disease: progress and problems on the road to therapeutics, Science 297 (2002) 353–356.
[2] C. Haass, D.J. Selkoe, Soluble protein oligomers in neurodegeneration: lessons from the Alzheimer's amyloid beta-peptide, Nat Rev. Mol. Cell Biol 8 (2007) 101–112.
[3] K.G. Mawuenyega, W. Sigurdson, V. Ovod, L. Munsell, T. Kasten, J.C. Morris, K. E. Yarasheski, R.J. Bateman, Decreased clearance of CNS beta-amyloid in Alzheimer's disease, Science 330 (2010) 1774.
[4] H. Cynis, J.L. Frost, H. Crehan, C.A. Lemere, Immunotherapy targeting pyroglutamate-3 Abeta: prospects and challenges, Mol. Neurodegener. 11 (2016) 48.
[5] C.A. Lemere, E. Masliah, Can Alzheimer disease be prevented by amyloid-beta immunotherapy? Nat. Rev. Neurol. 6 (2010) 108–119.
[6] W.M. Pardridge, Brain drug targeting and gene technologies, Jpn. J. Pharmacol. 87 (2001) 97–103.
[7] W.M. Pardridge, Blood-brain barrier drug targeting: the future of brain drug development, Mol. Interv. 3 (2003) 90–105 (151).
[8] A.M. Chacko, C. Li, D.A. Pryma, S. Brem, G. Coukos, V. Muzykantov, Targeted delivery of antibody-based therapeutic and imaging agents to CNS tumors: crossing the blood-brain barrier divide, Expert. Opin. Drug Deliv 10 (2013) 907–926.
[9] K. Hynynen, N. McDannold, N. Vykhodtseva, F.A. Jolesz, Noninvasive MR imaging-guided focal opening of the blood-brain barrier in rabbits, Radiology 220 (2001) 640–646.
[10] M. Aryal, C.D. Arvanitis, P.M. Alexander, N. McDannold, Ultrasound-mediated blood-brain barrier disruption for targeted drug delivery in the central nervous system, Adv. Drug Deliv. Rev. 72 (2014) 94–109.
[11] J.F. Jordao, C.A. Ayala-Grosso, K. Markham, Y. Huang, R. Chopra, J. McLaurin, K. Hynynen, I. Aubert, Antibodies targeted to the brain with image-guided focused ultrasound reduces amyloid-beta plaque load in the TgCRND8 mouse model of Alzheimer's disease, PLoS One 5 (2010), e10549.
[12] M. Liu, S. Jevtic, K. Markham-Coultes, N.P.K. Ellens, M.A. O'Reilly, K. Hynynen, I. Aubert, J. McLaurin, Investigating the efficacy of a combination Abeta-targeted treatment in a mouse model of Alzheimer's disease, Brain Res. 1678 (2018) 138–145.
[13] P.H. Hsu, Y.T. Lin, Y.H. Chung, K.J. Lin, L.Y. Yang, T.C. Yen, H.L. Liu, Focused ultrasound-induced blood-brain barrier opening enhances GSK-3 inhibitor delivery for amyloid-Beta plaque reduction, Sci. Rep. 8 (2018) 12882.
[14] J.F. Jordao, E. Thevenot, K. Markham-Coultes, T. Scarcelli, Y.Q. Weng, K. Xhima, M. O'Reilly, Y. Huang, J. McLaurin, K. Hynynen, I. Aubert, Amyloid-beta plaque reduction, endogenous antibody delivery and glial activation by brain-targeted, transcranial focused ultrasound, Exp. Neurol. 248 (2013) 16–29.
[15] A. Burgess, S. Dubey, S. Yeung, O. Hough, N. Eterman, I. Aubert, K. Hynynen, Alzheimer disease in a mouse model: MR imaging-guided focused ultrasound targeted to the hippocampus opens the blood-brain barrier and improves pathologic abnormalities and behavior, Radiology 273 (2014) 736–745.
[16] G. Leinenga, J. Gotz, Scanning ultrasound removes amyloid-beta and restores memory in an Alzheimer's disease mouse model, Sci. Transl. Med. 7 (2015) 278ra233.
[17] G. Leinenga, J. Gotz, Safety and efficacy of scanning ultrasound treatment of aged APP23 mice, Front. Neurosci. 12 (2018) 55.
[18] N. Lipsman, Y. Meng, A.J. Bethune, Y. Huang, B. Lam, M. Masellis, N. Herrmann, C. Heyn, I. Aubert, A. Boutet, G.S. Smith, K. Hynynen, S.E. Black, Blood-brain barrier opening in Alzheimer's disease using MR-guided focused ultrasound, Nat. Commun. 9 (2018) 2336.
[19] J.L. Frost, K.X. Le, H. Cynis, E. Ekpo, M. Kleinschmidt, R.M. Palmour, F.R. Ervin, S. Snigdha, C.W. Cotman, T.C. Saido, R.J. Vassar, P. George-Hyslop, T. Ikezu, S. Schilling, H.U. Demuth, C.A. Lemere, Pyroglutamate-3 amyloid-beta deposition in the brains of humans, non-human primates, canines, and Alzheimer disease-like transgenic mouse models, Am. J. Pathol. 183 (2013) 369–381.
[20] J.L. Frost, B. Liu, M. Kleinschmidt, S. Schilling, H.U. Demuth, C.A. Lemere, Passive immunization against pyroglutamate-3 amyloid-beta reduces plaque burden in Alzheimer-like transgenic mice: a pilot study, Neurodegener. Dis. 10 (2012) 265–270.
[21] J.L. Frost, B. Liu, J.U. Rahfeld, M. Kleinschmidt, B. O'Nuallain, K.X. Le, I. Lues, B. J. Caldarone, S. Schilling, H.U. Demuth, C.A. Lemere, An anti-pyroglutamate-3 Abeta vaccine reduces plaques and improves cognition in APPswe/PS1DeltaE9 mice, Neurobiol. Aging 36 (2015) 3187–3199.
[22] H. Crehan, B. Liu, M. Kleinschmidt, J.U. Rahfeld, K.X. Le, B.J. Caldarone, J.L. Frost, T. Hettmann, B. Hutter-Paier, B. O'Nuallain, M.A. Park, M.F. DiCarli, I. Lues, S. Schilling, C.A. Lemere, Effector function of anti-pyroglutamate-3 Aβ antibodies affects cognitive benefit, glial activation and amyloid clearance in Alzheimer's-like mice, Alzheimers Res. Ther. 12 (2020) 12.
[23] T. Hettmann, S.D. Gillies, M. Kleinschmidt, A. Piechotta, K. Makioka, C.A. Lemere, S. Schilling, J.U. Rahfeld, I. Lues, Development of the clinical candidate PBD-C06, a

humanized pGlu3-Aβ-specific antibody against Alzheimer's disease with reduced complement activation, Sci. Rep. 10 (2020) 3294.
[24] K.R. Kleinknecht, B.T. Bedenk, S.F. Kaltwasser, B. Grunecker, Y.C. Yen, M. Czisch, C.T. Wotjak, Hippocampus-dependent place learning enables spatial flexibility in C57BL6/N mice, Front. Behav. Neurosci. 6 (2012) 87.
[25] L. Alonso-Nanclares, P. Merino-Serrais, S. Gonzalez, J. DeFelipe, Synaptic changes in the dentate gyrus of APP/PS1 transgenic mice revealed by electron microscopy, J. Neuropathol. Exp. Neurol. 72 (2013) 386–395.
[26] C.A. Dickey, J.F. Loring, J. Montgomery, M.N. Gordon, P.S. Eastman, D. Morgan, Selectively reduced expression of synaptic plasticity-related genes in amyloid precursor protein + presenilin-1 transgenic mice, J. Neurosci. 23 (2003) 5219–5226.
[27] M.J. West, G. Bach, A. Soderman, J.L. Jensen, Synaptic contact number and size in stratum radiatum CA1 of APP/PS1DeltaE9 transgenic mice, Neurobiol. Aging 30 (2009) 1756–1776.
[28] Q. Shi, S. Chowdhury, R. Ma, K.X. Le, S. Hong, B.J. Caldarone, B. Stevens, C. A. Lemere, Complement C3 deficiency protects against neurodegeneration in aged plaque-rich APP/PS1 mice, Sci. Transl. Med. 9 (2017).
[29] L. Zuroff, D. Daley, K.L. Black, M. Koronyo-Hamaoui, Clearance of cerebral Abeta in Alzheimer's disease: reassessing the role of microglia and monocytes, Cell. Mol. Life Sci. 74 (2017) 2167–2201.
[30] M.A. Mintun, A.C. Lo, C. Duggan Evans, A.M. Wessels, P.A. Ardayfio, S. W. Andersen, S. Shcherbinin, J. Sparks, J.R. Sims, M. Brys, L.G. Apostolova, S. P. Salloway, D.M. Skovronsky, Donanemab in early Alzheimer's disease, N. Engl. J. Med. 384 (2021) 1691–1704.
[31] S. Dubey, S. Heinen, S. Krantic, J. McLaurin, D.R. Branch, K. Hynynen, I. Aubert, Clinically approved IVIg delivered to the hippocampus with focused ultrasound promotes neurogenesis in a model of Alzheimer's disease, Proc. Natl. Acad. Sci. U. S. A. 117 (2020) 32691–32700.
[32] M.A. O'Reilly, R.M. Jones, E. Barrett, A. Schwab, E. Head, K. Hynynen, Investigation of the safety of focused ultrasound-induced blood-brain barrier opening in a natural canine model of aging, Theranostics 7 (2017) 3573–3584.
[33] F. Kosel, J.M.S. Pelley, T.B. Franklin, Behavioural and psychological symptoms of dementia in mouse models of Alzheimer's disease-related pathology, Neurosci. Biobehav. Rev. 112 (2020) 634–647.
[34] C. Janus, A.Y. Flores, G. Xu, D.R. Borchelt, Behavioral abnormalities in APPSwe/PS1dE9 mouse model of AD-like pathology: comparative analysis across multiple behavioral domains, Neurobiol. Aging 36 (2015) 2519–2532.
[35] R.B. Demattos, J. Lu, Y. Tang, M.M. Racke, C.A. Delong, J.A. Tzaferis, J.T. Hole, B. M. Forster, P.C. McDonnell, F. Liu, R.D. Kinley, W.H. Jordan, M.L. Hutton, A plaque-specific antibody clears existing beta-amyloid plaques in Alzheimer's disease mice, Neuron 76 (2012) 908–920.
[36] R. Sperling, S. Salloway, D.J. Brooks, D. Tampieri, J. Barakos, N.C. Fox, M. Raskind, M. Sabbagh, L.S. Honig, A.P. Porsteinsson, I. Lieberburg, H.M. Arrighi, K.A. Morris, Y. Lu, E. Liu, K.M. Gregg, H.R. Brashear, G.G. Kinney, R. Black, M. Grundman, Amyloid-related imaging abnormalities in patients with Alzheimer's disease treated with bapineuzumab: a retrospective analysis, Lancet Neurol. 11 (2012) 241–249.
[37] M. Irizarry, J. Sims, S. Lowe, A. Nakano, B. Willis, C. Gonzales, S. Fujimoto, D. RA, K. RJ, S. Shcherbinin, A. Schwartz, M. Mintun, M. Devous Sr., R. DeMattos, Safety, pharmacokinetics (PK), and Florbetapir F-18 positron emission tomography (PET) after multiple dose administration of LY3002813, a B-amyloid plaque-specific antibody, in: Alzheimer's disease (AD), Proc. Alzheimer's Association International Conference (AAIC), 2016.
[38] S. Schilling, J.U. Rahfeld, I. Lues, C.A. Lemere, Passive abeta immunotherapy: current achievements and future perspectives, Molecules 23 (2018).
[39] D. Morgan, The role of microglia in antibody-mediated clearance of amyloid-beta from the brain, CNS. Neurol. Disord. Drug Targets 8 (2009) 7–15.
[40] C. Poon, C. Pellow, K. Hynynen, Neutrophil recruitment and leukocyte response following focused ultrasound and microbubble mediated blood-brain barrier treatments, Theranostics 11 (2021) 1655–1671.
[41] S. Knafo, L. Alonso-Nanclares, J. Gonzalez-Soriano, P. Merino-Serrais, I. Fernaud-Espinosa, I. Ferrer, J. DeFelipe, Widespread changes in dendritic spines in a model of Alzheimer's disease, Cereb. Cortex 19 (2009) 586–592.
[42] S. Hong, V.F. Beja-Glasser, B.M. Nfonoyim, A. Frouin, S. Li, S. Ramakrishnan, K. M. Merry, Q. Shi, A. Rosenthal, B.A. Barres, C.A. Lemere, D.J. Selkoe, B. Stevens, Complement and microglia mediate early synapse loss in Alzheimer mouse models, Science 352 (2016) 712–716.
[43] T. Sun, Y. Zhang, C. Power, P.M. Alexander, J.T. Sutton, M. Aryal, N. Vykhodtseva, E.L. Miller, N.J. McDannold, Closed-loop control of targeted ultrasound drug delivery across the blood-brain/tumor barriers in a rat glioma model, Proc Natl. Acad. Sci. U. S. A 114 (2017) E10281–E10290.
[44] Q. Shi, K.J. Colodner, S.B. Matousek, K. Merry, S. Hong, J.E. Kenison, J.L. Frost, K. X. Le, S. Li, J.C. Dodart, B.J. Caldarone, B. Stevens, C.A. Lemere, Complement C3-deficient mice fail to display age-related hippocampal decline, J. Neurosci. 35 (2015) 13029–13042.
[45] G.M. Leggio, S.A. Torrisi, F. Papaleo, The discrete paired-trial variable-delay T-maze task to assess working memory in mice, Bio Protocol 10 (2020), e3664.
[46] H. Shoji, H. Hagihara, K. Takao, S. Hattori, T. Miyakawa, T-Maze forced alternation and left-right discrimination tasks for assessing working and reference memory in mice, Journal of visualized experiments 60 (2012) e3300.
[47] R.M. Deacon, J.N. Rawlins, T-maze alternation in the rodent, Nat. Protoc. 1 (2006) 7–12.
[48] D.M. Ippolito, C. Eroglu, Quantifying synapses: an immunocytochemistry-based assay to quantify synapse number, J. Vis. Exp 45 (2010) e2270.
[49] M. Jin, N. Shepardson, T. Yang, G. Chen, D. Walsh, D.J. Selkoe, Soluble amyloid beta-protein dimers isolated from Alzheimer cortex directly induce tau hyperphosphorylation and neuritic degeneration, Proc Natl. Acad. Sci. U. S. A 108 (2011) 5819–5824.
[50] M. Maier, Y. Peng, L. Jiang, T.J. Seabrook, M.C. Carroll, C.A. Lemere, Complement C3 deficiency leads to accelerated amyloid beta plaque deposition and neurodegeneration and modulation of the microglia/macrophage phenotype in amyloid precursor protein transgenic mice, J. Neurosci. 28 (2008) 6333–6341.
[51] M.J. West, H.J. Gundersen, Unbiased stereological estimation of the number of neurons in the human hippocampus, J. Comp. Neurol. 296 (1990) 1–22.